Matrix Biology 35 (2014) 194–205

Contents lists available at ScienceDirect

Matrix Biology

journal homepage: www.elsevier.com/locate/matbio

Decorin deficiency promotes hepatic carcinogenesis

Zsolt Horváth [a], Ilona Kovalszky [a], Alexandra Fullár [a], Katalin Kiss [a], Zsuzsa Schaff [b], Renato V. Iozzo [c], Kornélia Baghy [a,*]

[a] 1st Department of Pathology and Experimental Cancer Research, Semmelweis University, Budapest, Hungary
[b] 2nd Department of Pathology, Semmelweis University, Budapest, Hungary
[c] Department of Pathology, Anatomy, and Cell Biology, and the Cancer Cell Biology and Signaling Program, Kimmel Cancer Center, Thomas Jefferson University, Philadelphia, PA, USA

ARTICLE INFO

Available online 18 December 2013

Keywords:
Small leucine-rich proteoglycan
Hepatocarcinogenesis
Receptor tyrosine kinase
MSPR/RON
c-Myc
β-Catenin
Cell signaling

ABSTRACT

Hepatocellular carcinoma represents one of the most-rapidly spreading cancers in the world. In the majority of cases, an inflammation-driven fibrosis or cirrhosis precedes the development of the tumor. During malignant transformation, the tumor microenvironment undergoes qualitative and quantitative changes that modulate the behavior of the malignant cells. A key constituent for the hepatic microenvironment is the small leucine-rich proteoglycan decorin, known to interfere with cellular events of tumorigenesis mainly by blocking various receptor tyrosine kinases (RTK) such as EGFR, Met, IGF-IR, PDGFR and VEGFR2. In this study, we characterized cell signaling events evoked by decorin deficiency in two experimental models of hepatocarcinogenesis using thioacetamide or diethyl nitrosamine as carcinogens. Genetic ablation of decorin led to enhanced tumor occurrence as compared to wild-type animals. These findings correlated with decreased levels of the cyclin-dependent kinase inhibitor $p21^{WAF1/CIP1}$ and a concurrent elevation in retinoblastoma protein phosphorylation via cyclin dependent kinase 4. Decreased steady state $p21^{Waf1/Cip1}$ levels correlated with enhanced expression of transcription factor AP4, a known transcriptional repressor of $p21^{Waf1/Cip1}$, and enhanced c-Myc protein levels. In addition, translocation of β-catenin was a typical event in diethyl nitrosamine-evoked tumors. In parallel, decreased phosphorylation of both c-Myc and β-catenin was observed in $Dcn^{-/-}$ livers likely due to the hindered GSK3β-mediated targeting of these proteins to proteasomal degradation. We discovered that in a genetic background lacking decorin, four RTKs were constitutively activated (phosphorylated), including three known targets of decorin such as PDGFRα, EGFR, IGF-IR, and a novel RTK MSPR/RON. Our findings provide powerful genetic evidence for a crucial in vivo role of decorin during hepatocarcinogenesis as lack of decorin in the liver and hepatic stroma facilitates experimental carcinogenesis by providing an environment devoid of this potent pan-RTK inhibitor. Thus, our results support future utilization of decorin as an antitumor agent in liver cancer.

1. Introduction

Hepatocellular carcinoma (HCC) represents the most frequent type of primary liver tumors, and it is the third most common fatal malignancy disease worldwide (El-Serag and Rudolph, 2007). The highest HCC incidence and mortality are observed in Eastern Asia and central Africa, but its frequency has been rapidly increasing in Europe and in the United States in the last decades. The major risk factors are hepatitis B and C infection, aflatoxin B1 intake from contaminated food and excessive alcohol abuse (Llovet et al., 2003; Sherman, 2010). Primary HCC often evolves on cirrhotic or chronic inflammation induced fibrotic background, although this is not essential for tumor formation.

The extracellular matrix (ECM) is an acellular compartment of organs, made of macromolecules providing support for the cells, they embrace. It is a key participant in the tissue specific organization of cells and the establishment of their differentiated function. ECM together with the nonparenchymal cells creates the microenvironment for the parenchymal cells in the tissues. The phenotype and behavior of parenchymal cells are influenced by their interrelationship with the stromal elements in a great extent. However, not only differentiated, but also malignant phenotype is proved to be driven by the microenvironment of cancer cells, including hepatomas. Their growth, local invasion and metastatic ability all depend on their microenvironment.

During malignant transformation, the tumorous ECM undergoes qualitative and quantitative changes. As a result, the matrix is capable to provide the proper environment for tumor progression. Accordingly,

Abbreviations: SLRP, small leucine-rich proteoglycan; RTK, receptor tyrosine kinase; TA, thioacetamide; DEN, diethyl nitrosamine; HCC, hepatocellular carcinoma; $Dcn^{-/-}$, decorin null; WT, wild type; $p21^{WAF1/CIP1}$, cyclin-dependent kinase inhibitor p21; AP4, transcription factor AP4; Rb, retinoblastoma protein; GSK3β, Glycogen synthase kinase 3β; GS, glutamine synthetase; AFP, alpha fetoprotein; CDK4, cyclin dependent kinase 4; EGFR, epidermal growth factor receptor; IGF-IR, insulin-like growth factor receptor I; PDGFR, platelet-derived growth factor receptor; MSPR, macrophage stimulating protein receptor; ECM, extracellular matrix; MAPK, mitogen activated protein kinase; ERK1/2, extracellular signal regulated kinase 1/2.

* Corresponding author at: 1st Department of Pathology and Experimental Cancer Research, Semmelweis University, Üllői út 26., Budapest 1085, Hungary. Tel.: +36 1 459 1500x54405; fax: +36 1 317 1074.
E-mail address: kori@korb1.sote.hu (K. Baghy).

0945-053X/$ – see front matter © 2013 Elsevier B.V. All rights reserved.
http://dx.doi.org/10.1016/j.matbio.2013.11.004

in the last decade scientific activities have been directed toward the better understanding of the relationship between the tumor and its matrix.

Decorin is a member of the small leucine-rich proteoglycan (SLRP) gene family (Iozzo and Murdoch, 1996; Iozzo, 1999; Iozzo et al., 2011) that is expressed in the stroma of various forms of cancer (Iozzo and Cohen, 1993) and thus has been recently proposed to act as a guardian from the matrix (Neill et al., 2012b), in analogy to p53, the guardian of the genome. Although this proteoglycan is ubiquitously expressed, practically no cells of epithelial origin synthesize it. This implies that decorin is a mesenchyme-specific gene product and that it exerts its effects in a paracrine fashion on endothelial and epithelial cells including cancer cells. Functionally, soluble and matrix-bound decorin modulate various biological processes including collagen fibrillogenesis, wound healing, myogenesis, bone physiology, stem cell biology, immunity, angiogenesis and fibrosis (Reed and Iozzo, 2002; Robinson et al., 2005; Zhang et al., 2009; Seidler et al., 2011; Ichii et al., 2012; Neill et al., 2012a, 2013; Brandan and Gutierrez, 2013; Chen and Birk, 2013; Dunkman et al., 2013; Sofeu Feugaing et al., 2013). Initially identified as a natural inhibitor of transforming growth factor-β (Yamaguchi et al., 1990; Ruoslahti and Yamaguchi, 1991), soluble decorin is emerging as a pan-RTK inhibitor targeting a multitude of RTKs with various affinities, including EGFR, Met, IGF-IR, VEGFR2 and PDGFR (Iozzo, 1999; Schonherr et al., 2005; Schaefer et al., 2007; Goldoni et al., 2009; Iozzo et al., 2011; Khan et al., 2011; Nikitovic et al., 2012; Schaefer and Iozzo, 2012; Seidler, 2012; Baghy et al., 2013; Buraschi et al., 2013; Morrione et al., 2013). Besides initiating signaling, this decorin/RTK interaction can induce caveosomal internalization and receptor degradation (Zhu et al., 2005).

Notably, a combined genetic ablation of decorin and of the tumor suppressor p53 induces the formation of early and aggressive T-cell lymphomas that lead to a premature demise of the compound mice (Iozzo et al., 1999a). These genetic studies are further supported by genetic evidence where loss of the decorin gene is permissive for tumorigenic growth of intestinal tumors with a concurrent increase in the levels of β-catenin (Bi et al., 2008, 2012). Conversely, decorin delivered via adenoviral-mediated gene transduction or systemic administration of recombinant protein to several tumor xenografts, such as breast and prostate carcinomas, inhibits tumorigenic growth (Reed et al., 2002, 2005; Tralhao et al., 2003; Araki et al., 2009; Hu et al., 2009; Buraschi et al., 2012).

A healthy liver contains only a small amount of decorin deposited around the central veins and portal tracts. However, an increased deposition of decorin was observed in the connective tissue septa during fibrogenesis (Dudas et al., 2001; Baghy et al., 2011). In hepatocellular carcinoma, deregulation of several signaling pathways has been described involving RAS/MAPK, IGF, HGF/MET, WNT/β-catenin, EGFR, VEGFR and PDGFR (Villanueva et al., 2007). The observation that decorin affects multiple signaling pathways emanating from various RTKs together with its ability to downregulate β-catenin and Myc levels (Buraschi et al., 2010) and to concurrently induce $p21^{WAF1/CIP1}$ (Santra et al., 1997), prompted us to investigate the role of decorin in mouse models of hepatocarcinogenesis evoked by TA or DEN. We found that a genetic background lacking one single SLRP caused a constitutive activation of various RTKs thus providing a mechanistic explanation for the increased incidence of hepatocellular carcinomas in decorin-null livers following experimental carcinogenesis.

2. Results

2.1. Decorin-null mice are more susceptible to experimentally-induced liver cancer

Metabolization of thioacetamide (TA) in hepatocytes via cytochrome p450 causes fibrosis, and subsequently hepatic cirrhosis. Thus, chronic TA exposure provokes hyper-regeneration of hepatocytes initiating hepatocarcinogenesis in the cirrhotic liver (Becker, 1983; Camus-Randon et al., 1996) (Fig. 1A,B). TA-induced tumors showed abundant cytoplasm with strong eosinophilic staining, and were surrounded by a connective tissue capsule. In contrast, high dose of diethyl nitrosamine (DEN) causes DNA mutations directly without evoking overt fibrotic changes (Heindryckx et al., 2009) (Fig. 1C,D). These tumor cells had narrow basophilic cytoplasm, and often invaded blood vessels.

Thioacetamide treatment induced liver tumor in ~93% of the mice lacking the decorin gene in contrast to only ~22% tumor prevalence observed in wild-type counterparts ($n = 15$ each, $p < 0.001$, Fig. 1E). Moreover, $Dcn^{-/-}$ mice developed more tumors upon DEN treatment as compared to wild type (44% vs. 27%) (Fig. 1F), although the difference did not reach statistical significance ($n = 10$, $p = 0.12$). In parallel, significantly higher tumor volume was calculated in $Dcn^{-/-}$ animals than that of wild type ones treated with TA (100.4 mm^3 vs. 7.6 mm^3 respectively ($p < 0.01$)) as well as DEN (23.7 mm^3 tumor volume in knockout and 3.4 mm^3 in wild type mice) (Fig. 1G). Thus, ablation of decorin sensitizes liver for tumor formation, and this effect is more pronounced in hepatocarcinogenesis with a cirrhotic background such as that induced by TA.

2.2. Qualitative and quantitative changes of decorin in TA- and DEN-induced tumors

Under unchallenged conditions, decorin was primarily located in the peri-portal areas and around the central veins of the liver (Fig. 2A,B). As thioacetamide induces cirrhosis and thus a stromal activation, the amount of decorin seemed to be increased in TA-treated livers of wild type animals as detected by immunostaining (Fig. S1, Fig. 2C,D). Accumulation of decorin was seen in fibrotic septa, and focal deposits were also observed in the tumor stroma (Fig. 2C,D). The immunodistribution of decorin was overall similar in DEN- and TA-induced tumors (Fig. 2E, F). Tumor foci were surrounded by well-defined deposits of immunoreactive decorin. Interestingly, we observed not only quantitative changes but also qualitative changes in the glycanation of decorin. Unlike control samples where decorin appeared as a smear between 60 and 80 kDa, the proteoglycan in TA-treated livers was significantly retarded and centered at ~90 kDa (Fig. 2G). DEN exposure also caused a shift toward higher molecular mass, although to a lesser degree (Fig. 2G). Notably, quantification of several experiments showed a significant induction of high molecular weight decorin content in both experimental animal models ($p < 0.001$ and $p < 0.05$, respectively; Fig. 2H). These observations suggest that the expression of decorin is dynamically modulated during hepatic carcinogenesis, especially in the TA-driven tumors where the stroma plays a more prominent role than in DEN-driven tumors.

2.3. Lack of decorin accelerates cell cycle progression

Next, we investigated the status of the cyclin-dependent kinase inhibitor $p21^{Waf1/Cip1}$ since lack of decorin prevents its upregulation in TA-induced liver cancer (Baghy et al., 2013). In control animals, low levels of $p21^{Waf1/Cip1}$ were detected by immunostaining with no appreciable differences between wild-type and decorin-deficient livers (Fig. S2). Upon TA treatment, a marked induction of $p21^{Waf1/Cip1}$ was observed in the wild-type samples (Fig. 3A, B). Hepatocytes, cells of the connective tissue and tumor cells displayed intense positive staining. In contrast, no accumulation could be detected in tumor cells lacking decorin gene (Fig. 3E, F). Diethyl nitrosamine increased the amount of $p21^{Waf1/Cip1}$ as well (Fig. 3C, D), but decorin deficiency had less impact on this process, as a considerable immunopositivity was observed in $Dcn^{-/-}$ tumor cell nuclei (Fig. 3G,H).

Next, we performed qPCR for the genes encoding $p21^{Waf1/Cip1}$ (*CDKN1A*) and the transcription factor AP4 (*TFAP4*), a c-MYC-inducible basic helix–loop–helix leucine-zipper transcription factor that represses *CDKN1A* expression. TA and DEN induced a 140-fold and a 20-fold elevation of *CDKN1A*, respectively, when compared to control samples

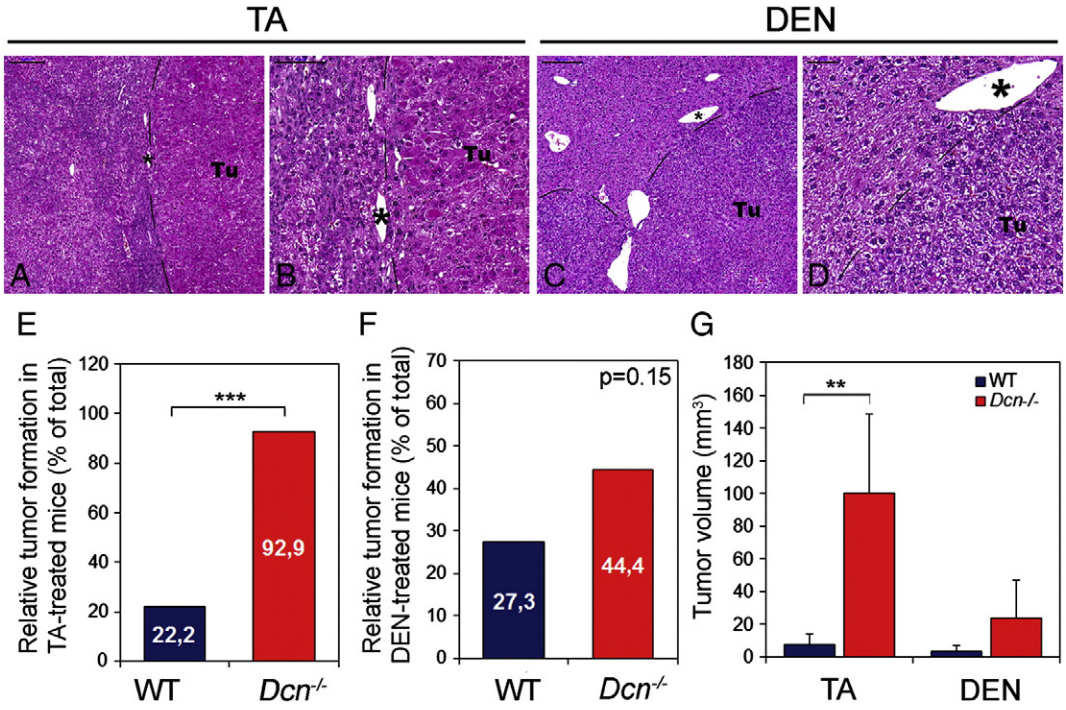

Fig. 1. Representative histological images of normal and tumorous livers induced by thioacetamide (TA) (A, B) or with diethyl nitrosamine (DEN) (C, D). Tu = tumor, dashed lines indicate tumor border. Asterisks show the same vein in different magnifications. Scale bar = 200 μm for A and C, 100 μm for B and D. Bar charts represent the ratios of tumor-bearing mice in experimental groups of wild-type and decorin gene knockout ($Dcn^{-}/^{-}$) mice with TA (E) and DEN treatment (F). N = 15 for TA and 10 for DEN-exposed groups. ***$p < 0.001$ (χ^2- test). (G) Columns represent the tumor volume measured in livers exposed to TA and DEN. **$p < 0.01$. All data are expressed as mean ± SD.

(Fig. 3I). Notably, significantly lower basal levels of *CDKN1A* gene expression were detected in the decorin-null samples, regardless of the carcinogen used ($p < 0.05$). In support of these data, we found a significant enhancement of *TFAP4* gene expression in decorin-deficient livers when compared to wild type specimens ($p < 0.01$, Fig. 3J). TA and DEN treatment decreased the level of AP4 in wild type animals by 52% and 17% respectively. Thus, decorin deficiency leads to a marked arrest of *CDKN1A* expression during experimental carcinogenesis, especially following TA treatment, with a concurrent induction of *TFAP4*.

To determine the exact point where $p21^{Waf1/Cip1}$ interfered with the cell cycle in our experimental model, different phosphorylation sites of the retinoblastoma protein (Rb) were checked by immunoblotting with

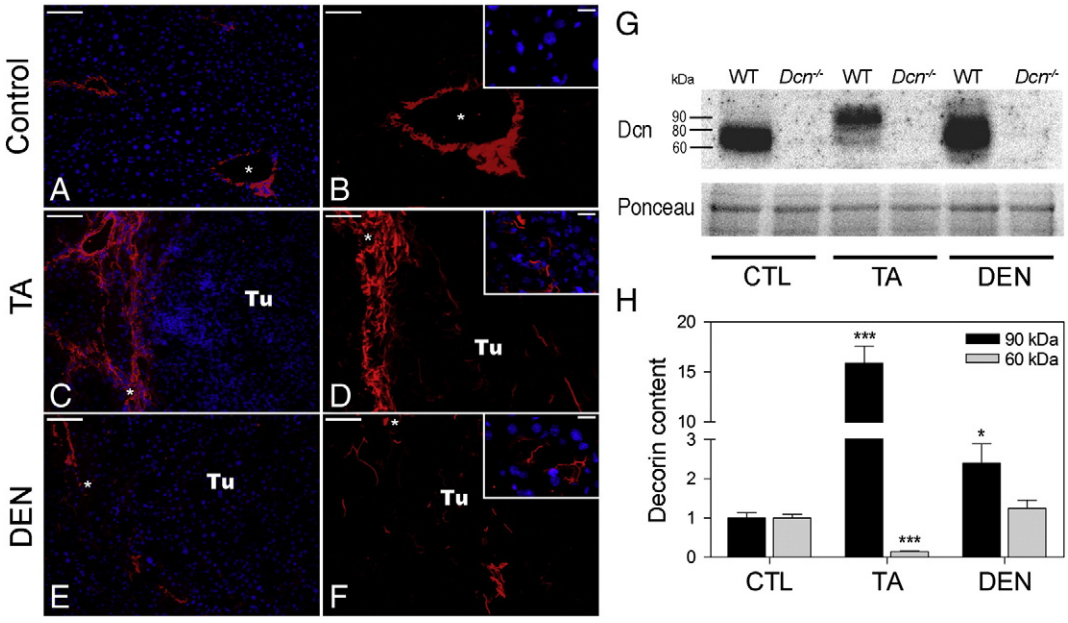

Fig. 2. Changes of decorin level and localization in liver cancer. Immunostaining of decorin proteoglycan (red) in control (A, B), thioacetamide (TA) (C, D) and diethyl nitrosamine (E–F) exposed liver sections. Insets represent pictures taken within the tumor. Nuclei were counterstained with DAPI. Tu = tumor. Asterisks show the same part of sections with different magnifications. Scale bar = 100 μm for A, C and E, 50 μm for B, D and F, 15 μm for insets. Representative image of the Western blot membrane (G) with decorin immunostaining. Ponceau-staining was applied as loading control. (H) Diagrams show the decorin content at 2 different sizes in treated animals relative to control levels. Data are expressed as mean ± SD, *$p < 0.05$; ***$p < 0.001$.

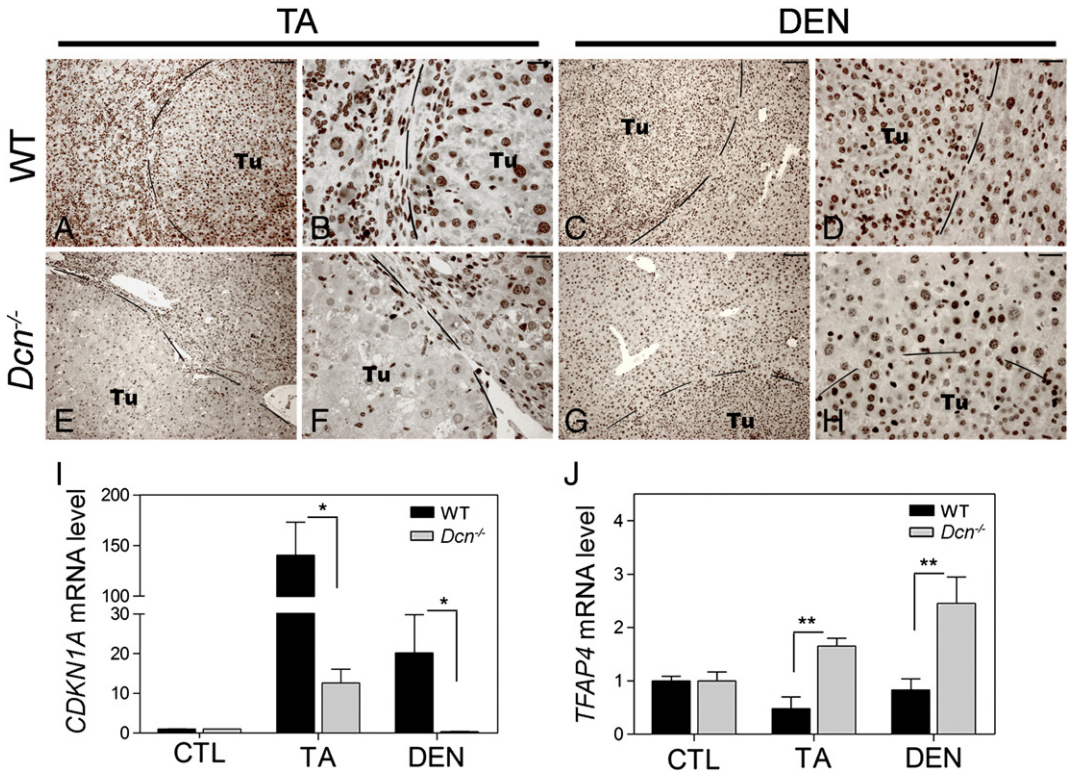

Fig. 3. Alterations in the p21$^{WAF1/CIP1}$ level in wild-type and decorin gene knockout ($Dcn^{-/-}$) mice n experimental hepatocarcinogenesis. Immunohistochemical analysis of p21$^{WAF1/CIP1}$ in tumorous liver sections after TA and DEN treatment in wild type mice (A–D) and in decorin-null ($Dcn^{-/-}$) mice (E-H). Tu = tumor. Dashed lines show tumor borders. Scale bar = 100 μm for A, C, E, G and 25 μm for B, D, F, H. Bar charts represent the relative *CDKN1A* (I) and *TFAP4* (J) mRNA levels in livers of wild-type (WT) and decorin knockout ($Dcn^{-/-}$) mice without treatment (control = CTL) and after TA or DEN exposure. Data are expressed as mean ± SD. *$p < 0.05$; **$p < 0.01$.

phospho-specific antibodies directed against either Ser780 or Thr821. Unlike control samples, TA-induced liver tumors showed a marked Rb phosphorylation at Ser780, known to be mediated through CDK4 activity, and this was more pronounced in the $Dcn^{-/-}$ samples vis-à-vis wild-type samples (2.65 vs. 1.77-fold, $p < 0.05$, Fig. 4A). DEN exposure resulted in 40% higher phospho-Rb at Ser780 level in decorin-null livers vis-à-vis wild type samples ($p < 0.05$, Fig. 4A,B). Rb phosphorylation at Thr821 is conducted exclusively by CDK2. Notably, tumors induced by

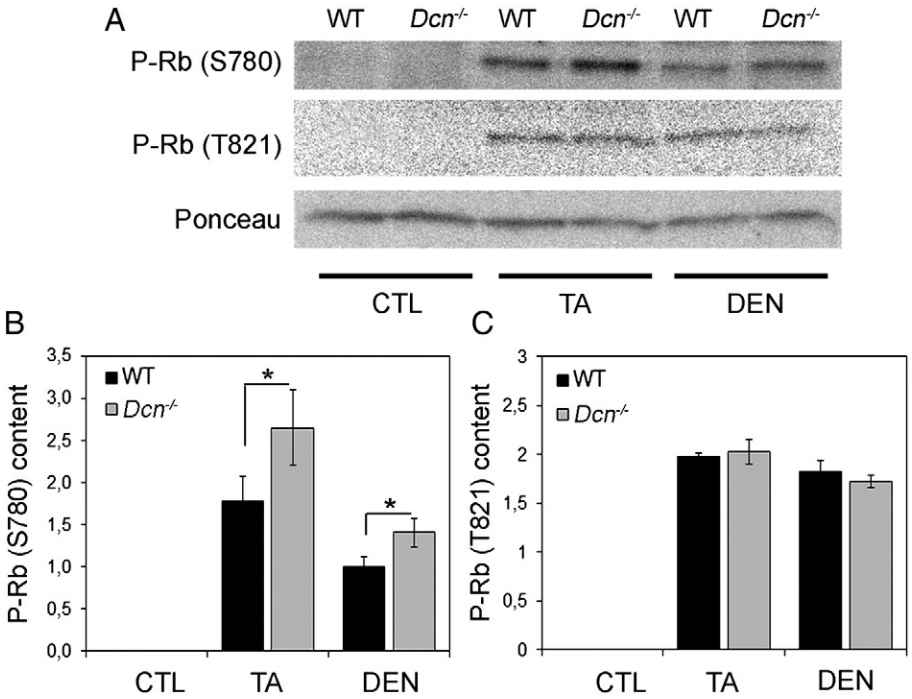

Fig. 4. Western blot analysis of retinoblastoma (Rb) phosphorylation at Ser780 and Thr821 in murine livers. Ponceau-staining was used as loading control (A). Bar charts show the relative content of P-Rb (S780) (B) and P-Rb (T821) (C) in lysates of wild-type (WT) and decorin deficient ($Dcn^{-/-}$) livers in control (CTL), TA and DEN-induced tumors. Data are expressed as mean ± SD. *$p < 0.05$.

either TA or DEN showed markedly elevated levels of P-Rb at Thr821, but decorin deficiency did not affect this process (Fig. 4A, C). We conclude that a genetic background deprived of decorin favors cell cycle progression of HCC by repressing AP4, inducing $p21^{Waf1/Cip1}$, and enhancing phosphorylation of P-Rb at Ser780 by CDK4/CyclinD complex. This series of events provides a mechanistic explanation for cells to bypass the restriction point at G1 and ultimately to affect cancer growth.

2.4. Major signaling pathways in HCC developed in a decorin-null background

Next, we aimed to identify signaling pathways leading to enhanced cell cycle progression in the HCC generated in decorin-null background. To this end, we investigated several key signaling molecules known to play important roles in hepatocarcinogenesis.

2.4.1. Changes of c-Myc

In normal liver, weak immunopositivity of c-Myc was detected both in the cytoplasm and the nucleus (Fig. S2,E–H). Under basal conditions, i.e., without exposure to carcinogens, decorin-deficient livers showed a ~40% elevation in the amount of c-Myc ($p < 0.01$, Fig. S3A). Both TA and DEN induced robust nuclear accumulation of c-Myc in both genotypes as well (Fig. 5A–H), showing no difference in the strength of nuclear staining between tumor cells and hepatocytes of the non-tumorous region. In addition, in wild-type livers exposed to TA, an intensive cytoplasmic c-Myc reaction was seen both in the tumor and in the

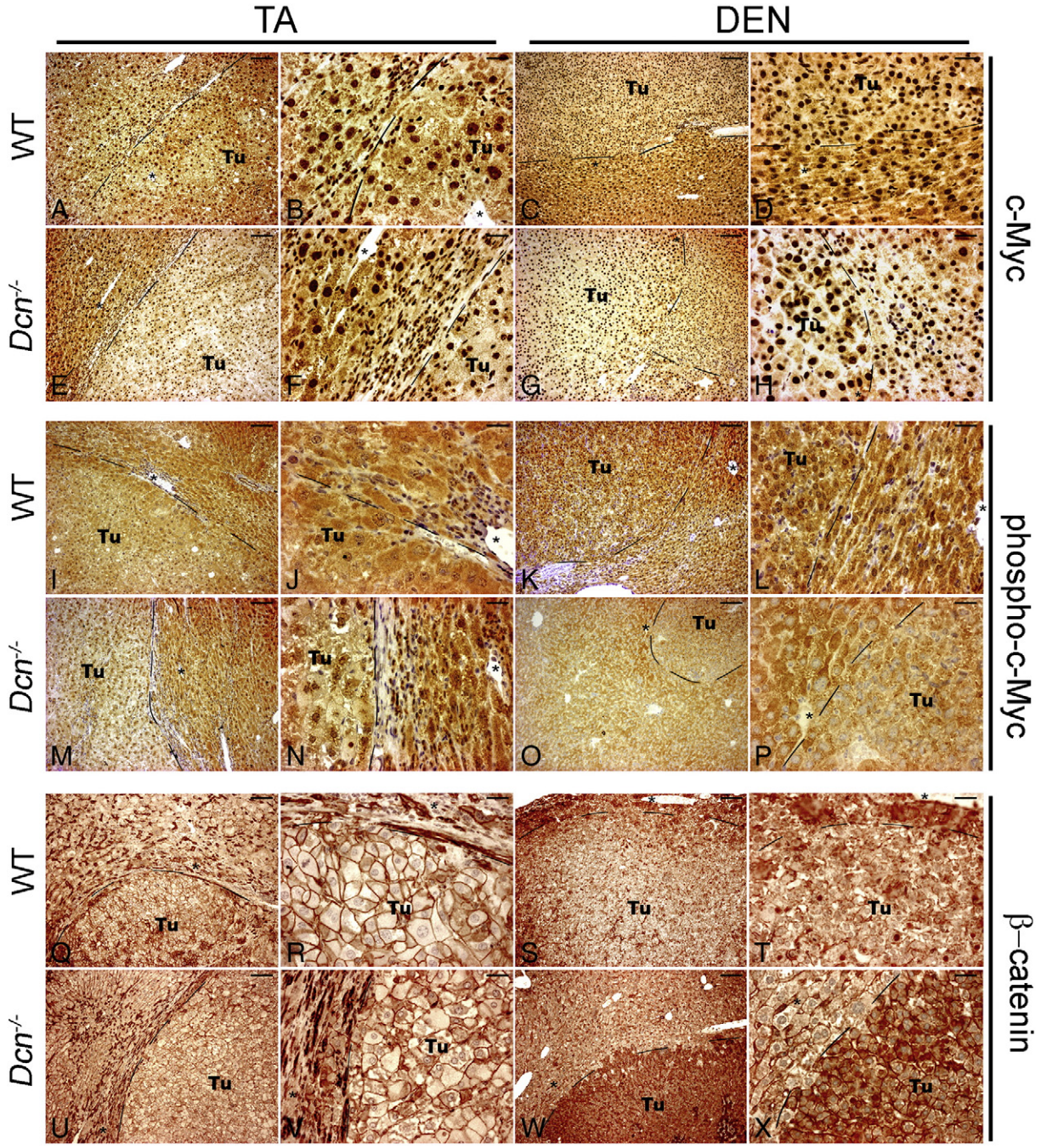

Fig. 5. Immunohistochemical analysis of various signaling proteins in wild-type (WT) and decorin-null liver tumors ($Dcn^{-/-}$) induced by TA or DEN. Representative images of c-Myc (A–H), phospho-c-Myc (I–P) and β-catenin (Q–X). Tu = tumor; dashed lines indicate tumor borders. Asterisks represent the same part of the sections with different magnifications. Scale bar = 100 μm for A, C, E, G, I, K, M, O, Q, S, U, and W and 25 μm for B, D, F, H, J, L, N, P, R, T, V, and X.

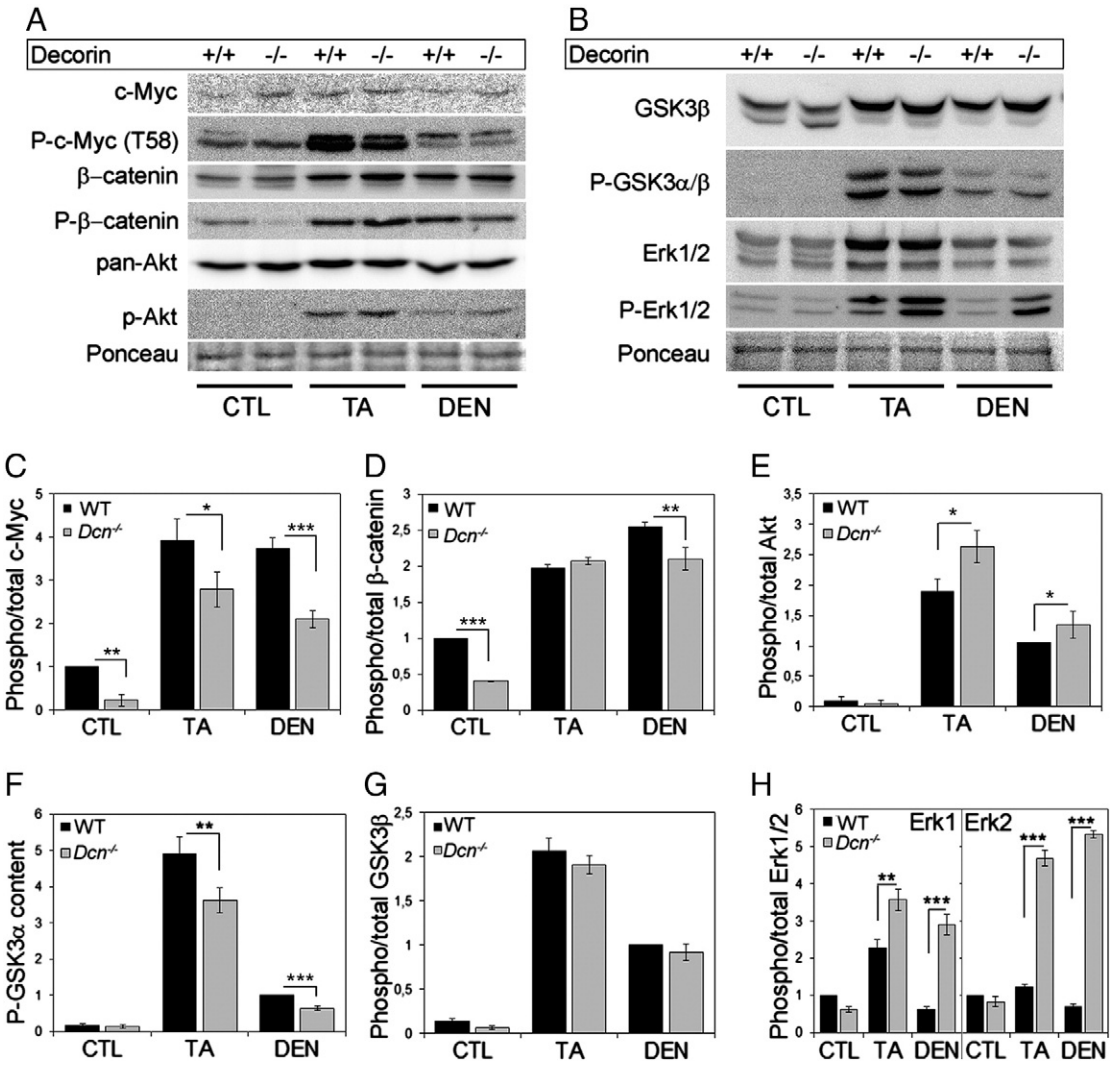

Fig. 6. Representative images of Western blot membranes probed for different signaling proteins (A, B). Ponceau-staining was applied as the loading control. Bar charts show the relative levels of target proteins after densitometric analysis of the blots (C–K) normalized to Ponceau staining in livers of wild-type (WT) and decorin knockout ($Dcn^{-/-}$) animals without treatment (control = CTL), after TA or DEN exposure. Data are expressed as mean ± SD. *$p < 0.05$; **$p < 0.01$; ***$p < 0.001$.

surrounding cirrhotic tissue (Fig. 5A,B), which did not occur in the decorin-deficient tumor cells (Fig. 5E, F). On Western blots, TA exposure resulted in c-Myc protein increase by 1.44-fold in wild-type samples, while decorin-null livers exhibited a 1.87-fold change (Fig. 6A, Fig. S3A). In DEN-induced tumors of wild type animals, cytoplasmic c-Myc protein levels were less in tumor cell than that of the surrounding tissue (Fig. 5C,D), and the reaction decreased further in $Dcn^{-/-}$ sections (Fig. 5G,H). The total c-Myc level measured was 1.1 fold and 1.3 fold in wild type and $Dcn^{-/-}$ livers, respectively (Fig. 6A, Fig. S3A).

To understand the changes in c-Myc localization, we tested the level of phosphorylated c-Myc, which bears the signal of ubiquitination, thus resides in the cytoplasm. By immunostaining, strong cytoplasmic positivity of tumor and non-tumorous cells of wild type livers was observed, regardless of the type of treatment (Fig. 5I–L). In contrast, decorin-null tumor cells contained less phospho-protein compared to their surrounding tissue (Fig. 5M–P). These results were confirmed by quantification of Western blot analysis (Fig. 6A,C), showing decreased level of phospho-c-Myc in $Dcn^{-/-}$ samples by 78% in control, 29% in TA-treated and 44% in DEN-induced tumors relative to the total c-Myc level ($p < 0.05$) (Fig. 6A,C).

2.4.2. The role of β-catenin

In control livers of both genotypes β-catenin was localized in the membrane of hepatic cells (Fig. S2, M–P). Thioacetamide exposure increased the amount of β-catenin, as strong immunostaining was observed in the surrounding cirrhotic zones, especially within proliferating bile ducts (Fig. 5Q,R,U,V). However, hepatocytes and most of the tumor cells retained their membranous β-catenin localization in both genotypes, with the exception of a few cells displaying cytoplasmic or weak nuclear signals (Fig. 5Q,R,U,V). In contrast, DEN induced marked translocation of the protein into the nucleus. In addition an increase in cytoplasmic immunopositivity was also detected (Fig. 5S,T,W,X). Total protein amounts of β-catenin and its inactive phosphorylated form were determined by immunoblottings. Unlike the control livers, the total amount of β-catenin markedly increased both upon TA and DEN exposure (Fig. 6A and Fig. S3B). In $Dcn^{-/-}$ livers, significantly less inactive β-catenin phosphorylated at Ser33/37/41 was seen as compared to control (1 vs. 0.4-fold, $p < 0.001$, Fig. 6D) and in DEN-treated samples (2.6 vs. 2.1-fold, $p < 0.001$, Fig. 6D). In contrast, after TA exposure of $Dcn^{-/-}$ livers phospho-β-catenin level raised parallel with the increase of total β-catenin, thus the ratio of phosphorylated/total protein remained identical in $Dcn^{-/-}$ and wild type groups (Fig. 6D).

2.4.3. Activity of the Akt

Signal transduction mediated by Akt is known to play important roles in carcinogenesis. Thus, we tested whether the level of Akt and its active phosphorylated form would be altered in our experimental animal model. In all conditions, we found no appreciable changes in

total Akt (Fig. 6A and Fig. S3C). In control lysates the phospho-Akt was practically undetectable (Fig. 6A,E). However, upon TA and DEN exposure, its amount dramatically rose (Fig. 6A,E). Notably, decorin-deficient tumors exhibited significantly higher level of phospho-Akt than wild-type, ~40% and ~29% for TA- and DEN-driven tumors, respectively ($p < 0.05$, Fig. 6E). Thus, also Akt pathway is activated in the absence of decorin in this experimental animal model of hepatocarcinogenesis.

2.4.4. Behavior of glycogen synthase kinase 3β (GSK3β)

GSK3β represents an important intersection among different signaling pathways. In our experimental hepatocarcinogenesis model, the total amount of GSK3β did not change upon decorin gene inactivation in control and TA-treated groups, while DEN exposure resulted in 16% higher protein level in $Dcn^{-/-}$ samples vis-à-vis wild-type (Fig. S3,D). Inactive phosphorylated forms of GSK3α and β were also tested by immunoblottings (Fig. 6B). Both α and β phospho-form levels markedly increased upon TA treatment (Fig. 6B,F,G). $Dcn^{-/-}$ livers contained 27% less P-GSK3α than wild-type ($p < 0.01$, Fig. 6B,F). The same effect was detected in DEN exposed livers, as decorin deficiency led to 35% lower level of inactive GSK3α ($p < 0.001$). Interestingly, no difference in phospho-GSK3β level was revealed between the genotypes either in control or in carcinogen-treated groups; however, both TA and DEN significantly increased the level of the protein (Fig. 6B,G).

2.4.5. The key player Erk1/2

The most prominent changes in signaling occurred in Erk1/2. Total amount of Erk1 and Erk2 proteins increased by ~2.5-fold and ~1.7-fold after TA treatment respectively (Fig. S3, E,F). DEN exposure raised the amount of Erk1/2 to ~1.2-fold. No significant differences were seen between the genotypes (Fig. S3, E,F). In wild-type animals, only TA induced phosphorylation of Erk1/2 proteins, while DEN had no effect on its activation level (Fig. 6B,H). Compared to controls, phospho-Erk1 was 2.3-fold vs. 3.6-fold higher in WT and $Dcn^{-/-}$ TA exposed samples respectively ($p < 0.01$, Fig. 6H) relative to the total Erk1 amount. Thioacetamide induced a 4.7 fold increase in Erk2 activation in $Dcn^{-/-}$ livers in contrast to 1.24-fold detected in wild-type ($p < 0.001$, Fig. 6H). Unlike DEN-treated wild-type samples, $Dcn^{-/-}$ mice showed an activation of Erk1/2 as high as 2.9- and 5.3-fold, respectively ($p < 0.001$, Fig. 6H). Thus, Erk1/2 pathway is constitutively activated by a genetic background devoid of decorin.

2.5. Enhanced receptor tyrosine kinase activity in decorin-null mice

Next, we attempted to identify the putative receptors mediating the downstream signaling described above. To this end, we utilized antibody arrays specific for phospho-receptor tyrosine kinases which were successfully used before to detect Met as a novel ligand for decorin protein core (Goldoni et al., 2009) and several RTKs for endorepellin (Nystrom et al., 2009). We identified four RTKs, namely PDGFRα, EGFR, MSPR (also known as RON) and IGF-IR that exhibited significantly higher levels in response to the absence of decorin (Fig. 7). Notably, we found a 1.8 and 2.8 increase in tyrosine phosphorylation of PDGFRα in $Dcn^{-/-}$ TA- and DEN-driven tumors, respectively ($p < 0.001$, Fig. 7). Lack of decorin resulted in 1.5 and 3.6-times higher P-EGFR content for TA- and DEN-evoked tumors, respectively ($p < 0.05$, Fig. 7). We also found 1.4 and 1.9 increase in basal Tyr phosphorylation of MSPR (HGF-like growth factor receptor, RON) in $Dcn^{-/-}$ TA- and DEN-driven tumors ($p < 0.05$, Fig. 7). Interestingly, the amount of active c-Met receptor increased upon both carcinogen exposure, but decorin deficiency did not have any effect on the level of this RTK (data not shown). The phospho-IGF-IR was detected in a low amount in TA and DEN-induced tumors; however significantly higher quantities were measured in $Dcn^{-/-}$ livers than wild-type ($p < 0.05$, Fig. 7).

Collectively, our findings indicate that decorin deficiency results in higher activation of various RTKs that could drive tumor cell growth.

3. Discussion

Hepatocarcinogenesis is a multi-step process involving different genetic alterations and changes in signaling pathways that ultimately lead to malignant transformation of the hepatocytes (Farber, 1984). In addition, not only molecular events occurring in tumor cells, but also their interactions with macromolecules of the tumor microenvironment play a crucial role in tumor progression and metastasis (Daley et al., 2008; Marastoni et al., 2008; Hynes, 2009; Jarvelainen et al., 2009; Rozario and DeSimone, 2010; Hielscher et al., 2012). Based on the emerging evidence implicating decorin in the control of cell proliferation and growth factor/receptor interactions (Seidler and Dreier, 2008; Ferdous et al., 2010; Iozzo and Schaefer, 2010), we hypothesized that decorin could also play a key role during experimental hepatocarcinogenesis. In this study we utilized two well-established models of experimental primary hepatocarcinogenesis using TA and DEN as carcinogens. Thioacetamide is a promoter-type compound inducing fibrosis of the liver and a concurrent hyper-regeneration of hepatocytes resulting in liver cancer (Becker, 1983; Camus-Randon et al., 1996). Indeed, about 70% of human HCCs develop in cirrhotic livers. In contrast, diethyl nitrosamine represents a direct DNA mutagen that induces hepatic carcinomas without an intervening fibrotic remodeling (Heindryckx et al., 2009). At a molecular level, livers exposed to TA display highly elevated level of alpha-fetoprotein (AFP) (Fig. S4A). In contrast, DEN-induced tumors are characterized with high gluthamine synthetase (GS) expression (Fig. S4B), a target gene of β-catenin activity (Loeppen et al., 2002). Mutations of β-catenin and/or its translocation to the nucleus (Dahmani et al., 2011),

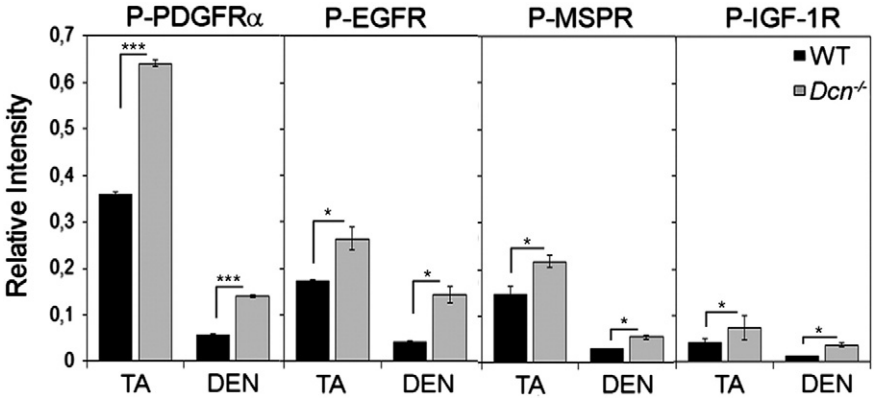

Fig. 7. Changes of various active receptor tyrosine kinases in TA and DEN-evoked primary liver cancer in wild-type and decorin gene-knockout ($Dcn^{-/-}$) mice. Diagrams represent the results obtained from densitometric analysis of array dots showing relative levels of phospho-PDGFRα, phospho-EGFR, phospho-MSPR, and phospho-IGF-IR normalized to the phospho-tyrosine positive control. Data are expressed as mean ± SD. *$p < 0.05$; ***$p < 0.001$.

as well as reactivation of AFP (Bertino et al., 2012), are typical and well-studied events of liver carcinogenesis. Moreover, expression analysis of 19 hepatoma cell lines revealed that AFP positive and β-catenin mutant cancer cells represent two different clusters of HCC confirming our observation on distinct expression of AFP and gluthamine synthetase in TA and DEN-induced tumors (Lee and Thorgeirsson, 2002). Changes in activation of key signaling molecules in the two types of carcinogenesis models corroborate to existence of two types of hepatocellular carcinoma as well. Overall, it seems that TA-induced tumors rather utilize the RTK/Ras/MAPK pathway, whereas DEN-induced tumors prefer the β-catenin activation.

Earlier, we reported that decorin deposits in fibrotic septa (Baghy et al., 2011), as well as around the invasive front of tumors and in the stroma induced by thioacetamide (Baghy et al., 2013). In this type of carcinogenesis we observed that the lack of decorin results in enhanced tumor formation in the liver. In parallel, we wondered whether the lack of decorin had any impact on the carcinogenesis induced in a non-cirrhotic background provoked by DEN. In such system, decorin deficiency led to a moderate enhancement in tumor prevalence and size, much less pronounced than that observed in TA-induced HCCs. In wild-type animals, not only the amount of decorin increases in HCCs, but also qualitative changes occur in decorin glycanation, likely due to a longer dermatan/chondroitin sulfate chain at the N-terminus. Notably, the decorin single glycosaminoglycan chain becomes progressively shorter with aging (Li et al., 2013). Thus, it is possible that the longer chain observed in the TA-induced tumors might be due to a more primitive fetal-like environment characteristic of various tumor stromas.

Regardless of the carcinogen agent used, the enhanced tumor formation observed in decorin-deficient livers is closely linked to a low induction of the potent cyclin-dependent kinase inhibitor $p21^{Waf1/Cip1}$ (Harper et al., 1993, 1995) detected at both mRNA and protein level. Notably, it is well established that soluble decorin protein core utilizes $p21^{Waf1/Cip1}$ to display its tumor repressor effect in most cases via both EGFR and Met (De Luca et al., 1996; Santra et al., 1997; Buraschi et al., 2010; Zhang et al., 2012). In our model system, lower $p21^{Waf1/Cip1}$ levels caused by decorin ablation resulted in higher activity of cyclin dependent kinase 4 as shown by enhanced retinoblastoma phosphorylation at Ser780. In parallel, the action of CDK2 remained unchanged upon decorin deficiency in neoplastic livers. Thus, our experimental data in mice correlate well with reports of enhanced level and activity of CKD4/CyclinD complexes in human HCCs (Jain et al., 2010; Rivadeneira et al., 2010; Lu et al., 2013).

Notably, decorin-null tumors showed increased expression of the transcription factor AP4, a known transcriptional repressor of $p21^{Waf1/Cip1}$ (Jung and Hermeking, 2009), thereby providing a mechanistic explanation for the down-regulation of $p21^{Waf1/Cip1}$ levels. We further tested the distribution and subcellular localization of c-Myc, a major transcription factor involved in the control of cell proliferation in a variety of cancers. The rationale for this line of research is based on the observation that soluble decorin and decorin protein core markedly downregulate c-Myc levels in a variety of cancer cell lines as well as in orthotopic mammary carcinoma xenografts (Buraschi et al., 2010; Iozzo and Sanderson, 2011; Neill et al., 2012b). In an agreement with these observations we detected robust nuclear accumulation of c-Myc in TA and DEN-evoked tumors in parallel with its decreased phosphorylation at Thr58, a post-translational modification known to destabilize c-Myc and target it for proteasomal degradation (Buraschi et al., 2010). In addition, c-Myc is a downstream target of β-catenin (He et al., 1998) that plays a crucial role in hepatocarcinogenesis. In our model system, translocation of β-catenin to the nucleus was observed in DEN-provoked tumors as well as elevated expression of GS reflecting on its efficiency. In contrast, TA exposure did not significantly alter the localization of the protein, and displayed lower levels of GS mRNA. Beside the canonical Wnt pathway, the action of β-catenin is known to be affected by several tyrosine kinases such as c-Met (Buraschi et al., 2010), RON (Danilkovitch-Miagkova et al., 2001) or EGFR (Hu and Li, 2010).

Decorin is known to modulate and interfere with signal transduction via binding to growth factors and their cognate receptors at the cell surface e.g. EGFR (Iozzo et al., 1999b; Csordas et al., 2000; Zhu et al., 2005), IGF-IR (Schonherr et al., 2005; Iozzo and Sanderson, 2011), Met (Goldoni et al., 2008). Earlier, we reported that PDGFRα activity is markedly elevated in TA-induced hepatocarcinogenesis in a decorin-deficient background (Baghy et al., 2013). However, in our extended dual liver carcinogenesis model, we observed significant basal Tyr phosphorylation (activation) in four RTKs, namely PDGFRα, EGFR, RON (MSPR) and IGF-IR upon decorin deficiency, regardless of the carcinogen used. It is notable that several of these RTKs have already been implicated in the pathogenesis of HCC in humans (Stock et al., 2007; Berasain et al., 2009; Oseini and Roberts, 2009; Wu and Zhu, 2011; Sengupta and Siddiqi, 2012; Chen et al., 2013). Surprisingly, no change in Tyr phosphorylation of Met was seen in decorin-deficient tumors, despite decorin's ability to interact with and downregulate this RTK. In our animal models we discovered that a novel RTK, not previously linked to decorin bioactivity, is MSPR, also called RON, the receptor for the hepatocyte growth factor-like protein. This is interesting insofar as RON has been implicated in the development and progression of human HCCs (Chen et al., 1997; Cho et al., 2011).

Downstream of RTKs, the Ras/MEK/ERK and PI3K/Akt/mTOR represent the major and most studied pathways in several types of cancers including HCC (Villanueva et al., 2007; Whittaker et al., 2010). We observed a striking elevation in Erk1/2 phosphorylation in the absence of decorin in liver tumors, even when it was not induced in wild-type animals upon DEN exposure. These changes were the most significant ones we observed upon ablation of decorin in our experimental set-up. In addition, phosphorylation of Akt markedly increased in $Dcn^{-/-}$ liver cancers when compared to that of wild-type animals. The active form of Akt is known to inactivate GSK3β via phosphorylation (Grimes and Jope, 2001; Jacobs et al., 2012). However, no difference in Phospho-GSK3β level between wild type and decorin-null liver tumors was seen by immunoblottings. Indeed, and in contrast to our prediction, decreased phosphorylation of c-Myc and β-catenin detected in the $Dcn^{-/-}$ carcinogen-exposed livers should reflect on the enhanced inactivation of GSK3β (Iozzo and Sanderson, 2011). Of note, GSK3β is a key molecule linking several signaling pathways such as those emanating from Wnt and RTKs. Thus, its activity is precisely regulated by various processes. Beside inactivating phosphorylation at Ser9, the action of GSK3β is enhanced by its phosphorylation at Tyr216. This activating phosphorylation is known to be hindered by EGF or insulin (Grimes and Jope, 2001). It is plausible that the decreased GSK3β function observed in decorin-null liver cancers is a result of its attenuated activating phosphorylation provoked by the higher activity of EGFR.

Decorin seems to be more effective in TA-induced liver cancer than in DEN-evoked one in non-cirrhotic background as its lack causes much pronounced tumorigenesis upon TA exposure when compared to wild type mice. We do not know whether collagen bound decorin is effective in interfering with signaling or associating with cell surface receptors. In cirrhotic liver decorin is accumulated along the fibrotic septa as well as around tumors, while there is much less decorin observed in DEN-induced HCCs. Of note, enhanced degradation of the extracellular matrix by MMPs is a typical process in both fibrogenesis (Dudas et al., 2001; Guo and Friedman, 2007) and carcinogenesis (Okazaki and Inagaki, 2012; Lempinen et al., 2013). As a consequence, we hypothesize that decorin could be released from collagens resulting in a local accumulation of the soluble proteoglycan at the invasive front of tumors. In this manner, as the amount of decorin already increased during cirrhosis, its local concentration around the tumors is much higher in HCCs with cirrhosis than in carcinomas developed in a non-cirrhotic surrounding leading to more pronounced tumor repression by decorin in TA-provoked cancer.

In conclusion, our novel findings indicate that a complex network of intervening cellular signaling events is present in our experimental hepatocarcinogenesis model. The ablation of decorin leads to enhanced

basal activation of PDGFRα, EGFR, RON and IGF-IR which would in concert transmit growth-promoting and pro-survival downstream signaling in an environment deplete of a powerful pan-RTK repressor. According to our working model (Fig. 8), the de-repression of several RTKs by a tumor stroma devoid of decorin would evoke a chronic activation of the Ras/MEK/ERK pathway, the main pathway of signal transduction found in our HCCs. In addition, Akt activation together with the observed hindered degradation of c-Myc and β-catenin provoked by decorin deficiency would play a contributing role as well (Fig. 8). Within the nucleus, c-Myc induces AP4 expression a known transcriptional repressor of $p21^{Waf1/Cip1}$. Consequently, reduced $p21^{Waf1/Cip1}$ levels would be insufficient to inactivate CDK4/CyclinD1. In this way, Rb phosphorylation would culminate in E2F release thereby allowing the cell to bypass the restriction point in G1 phase (Fig. 8).

Collectively, our findings provide novel information regarding the role of decorin in liver cancer and offer a mechanistic explanation for its in vivo biological activity. As decorin is a natural product, which has been detected in the circulation following sepsis and cancer (Merline et al., 2011) our results support the concept that decorin proteoglycan or protein core could be utilized in future studies as an antitumor agent useful in the battle against liver cancer.

4. Experimental procedures

4.1. Generation of decorin-null mice

All animal experiments were conducted according to the ethical standards of the Animal Health Care and Control Institute, Csongrád County, Hungary, permit No. XVI/03047-2/2008. Decorin deficient mice were generated as previously described (Danielson et al., 1997). In brief, the inactivation of the decorin gene was achieved by targeted disruption of the exon 2 inserting a PGK-Neo cassette. Two male and two female C57Bl/6 mice heterozygous for decorin gene ($Dcn^{-/-}$) which were backcrossed into C57Bl/6 background for nine generations, were bred until homozygosity. The genotype of the offspring was determined by PCR. Tail DNA was isolated by using high salt method. Subsequently 3 primers were applied, sense and antisense specific for the exon 2, and one corresponding to the PGK-Neo cassette. PCR products were analyzed by 2% agarose gel electrophoresis.

4.2. Induction of experimental hepatocarcinogenesis

For induction of liver cancer in a cirrhotic background, we utilized a total of 24 one month-old male mice. Fifteen wild-type, and 15 decorin-null ($Dcn^{-/-}$) animals with C57Bl/6 background were exposed to thioacetamide (TA) dissolved in drinking water (150 mg/l). To obtain fully-developed hepatocellular carcinoma, animals were subjected to TA treatment for 7 months. Age-matched untreated animals with identical genetic background served as controls. Mice were terminated after 7 months of thioacetamide exposure by cervical dislocation in ether anesthesia. Hepatocarcinogenesis in non-cirrhotic livers was induced by a single high-dose intraperitoneal injection of diethyl nitrosamine (DEN, 15 μg/g body weight) at the age of 15 days. Ten wild type and 10 $Dcn^{-/-}$ mice were utilized for this experiment and 5–5 age-matched untreated animals served as controls. Formation of hepatocellular carcinoma appeared 9 months after DEN injection. At termination, body weight and liver weight of the animals were measured and the number of macroscopically detectable tumors was counted. Half of the

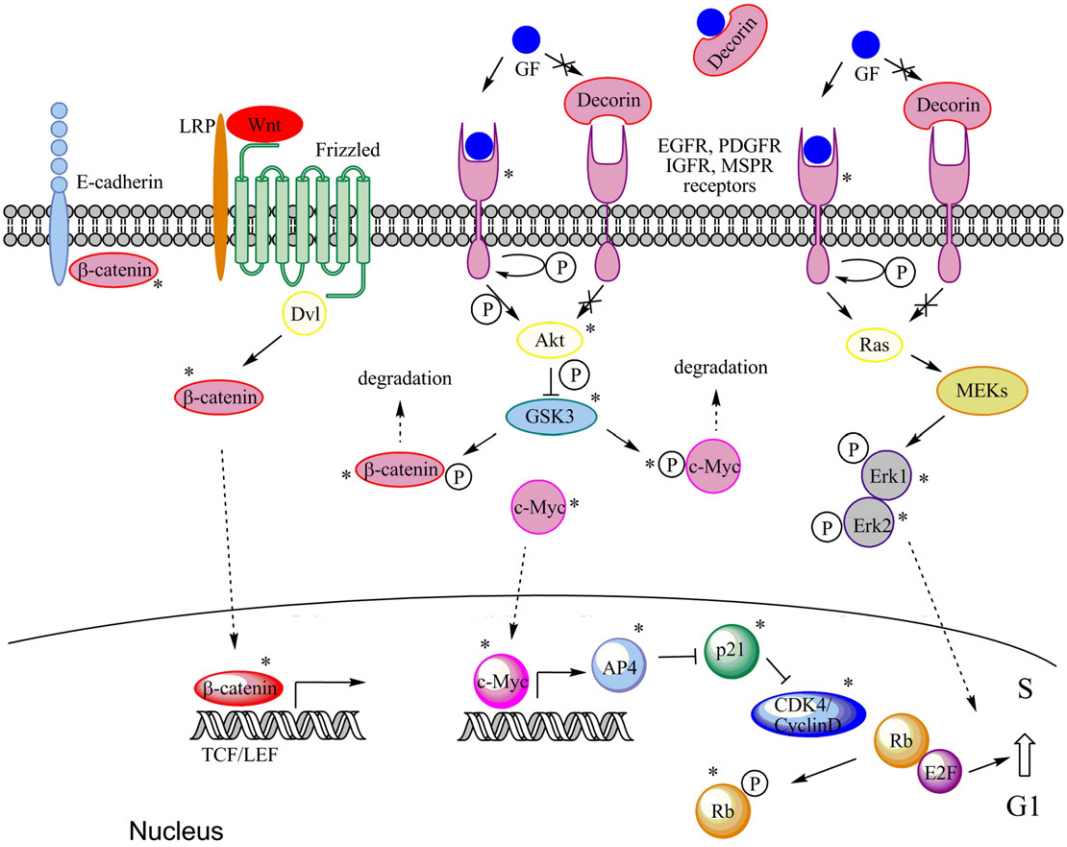

Fig. 8. Action of decorin on cellular signaling in experimental liver cancer. In the extracellular environment, decorin may bind to growth factors (such as PDGF) and various receptor tyrosine kinases (RTK). These interactions interfere with downstream signaling pathways, such as Akt/GSK3β or Ras/MEK/ERK. Changes in ERK1/2 in the presence or absence of decorin can be an outcome of crosstalk between the different growth factor receptors. The action of GSK3β leads to β-catenin and c-Myc degradation. Decorin utilizes $p21^{WAF1/CIP1}$ for cell-cycle blockade to display its tumor-repressor effect. When decorin is not present, c-Myc translocation to the nucleus induces the expression of AP4 that finally blocks $p21^{WAF1/CIP1}$. These events accumulate in enhanced retinoblastoma phosphorylation by CDK4 and push the cell cycle toward to S phase. GF = growth factor; GSK3 = glycogen synthase kinase 3; MEK, mitogen-activated protein kinase/ERK kinase.

liver samples were frozen for further processing and the other half was fixed in 10% formaldehyde and embedded in paraffin for histological analysis. Formalin-fixed paraffin-embedded sections were solubilized in xylene and stained with hematoxylin and eosin, or processed further for immunohistochemistry. Stained sections were used for histological diagnosis. To determine the tumor volume of livers, HE stained sections were scanned by Panoramic Scan (3D Histech Ltd., Budapest, Hungary). The length and width of tumors in each section were determined with the help of Pannoramic viewer program (3D Histech Ltd.) Tumor volume was calculated as $V = (\text{width (mm)})^2 \times \text{length (mm)}^*\pi) / 6$.

4.3. Real-time PCR (qPCR)

For qPCR, total RNA was isolated from frozen livers. After homogenization in liquid nitrogen total RNA was purified using the RNAeasy Mini Kit (Qiagen, Hilden, Germany), according to the protocol provided by the manufacturer. The yield and purity of RNA were estimated by an ND-1000 spectrophotometer (NanoDrop Technologies, Wilmington, DE, USA). The integrity and size distribution of the total RNA purified were analyzed using Experion RNA Chips and the Experion Automated Electrophoresis Station (Bio-Rad, Hercules, CA). Complementary DNAs (cDNAs) were generated from 1 μg of total RNA by M-MLV Reverse Transcriptase kit (Invitrogen by Life technologies Carlsbad, CA, USA) according to the instructions of the supplier. Real-time PCR was performed in an ABI Prism 7000 Sequence Detection System (Applied Biosystems by Life Technologies, Carlsbad, CA, USA), using ABI TaqMan Gene Expression Assays for mouse $p21^{WAF1/CIP1}$ (CDKN1A, Assay ID: Mm00432448_m1), AP4 (Assay ID: Mm00473137_m1), gluthamine synthetase (Assay ID: Mm00725701_s1), AFP (Mm00431715_m1) applying 18S rRNA as endogenous control (Part No. 4319413E) according to the manufacturer's protocol. All samples were run in duplicates in 20 μl total volume containing 50 ng cDNA using TaqMan Universal PCR Master Mix (Part No. 4324018, Applied Biosystems by Life Technologies). The thermal cycle conditions for reactions were as follows: denaturation for 10 min at 95 °C, 40 cycles of denaturation at 95 °C for 15 s and annealing at 60 °C for 1 min. Results were obtained as threshold cycle (C_T) values. Relative expression levels were calculated by using the $2^{-\Delta\Delta C}{}_T$ method.

4.4. Immunostaining

Formalin-fixed paraffin-embedded sections were solubilized in xylene and ethanol, then washed with distilled H_2O for 5 min. Antigen retrieval was performed in a pressure cooker using TRIS-EDTA buffer (10 mM TRIS, 1 mM EDTA, 0.05% Tween 20, pH 9) for 20 min. After cooling, slides were washed 3 times in PBS with 0.05% Tween20 (PBST). Next, endogenous peroxidase was inactivated by addition of 10% H_2O_2 dissolved in methanol for 10 min. After washing with PBST, 5 w/v% bovine serum albumin (BSA)/PBS containing10% normal serum was applied for 1 h to prevent any nonspecific binding. Primary antibodies were applied overnight at 4 °C. The next day, slides were washed 3 times in PBST, and then incubated with appropriate secondary antibodies conjugated either with horse reddish peroxidase or biotin for 1 h. A detailed list of primary and secondary antibodies and their appropriate dilutions is provided in Supplementary Table 1. For biotin-labeled secondary antibodies, signals were amplified by Vectastain ABC kit (Vector Laboratories, Burlingame, CA) following the instructions of the supplier. After washing, signals were visualized by using 3,3-diaminobenzidine tetrahydrochloride (DAB) substrate chromogen solution (Dako, Glostrup, Denmark) followed by counterstaining with hematoxylin. For decorin immunostaining, frozen sections of the liver were fixed in ice-cold methanol for 20 min. Next, slides were washed in PBS, blocked with 5 w/v% BSA/PBS containing 10 v/v% nonimmune serum of secondary antibody at 37 °C for 30 min. After washing, sections were incubated with the primary antibodies diluted in 1:50 in PBS containing 1 w/v% BSA, at 4 °C for 16 h. Appropriate fluorescent secondary antibodies were applied at room temperature for 30 min. Nuclei were stained with 4′-6′-diamidino-phenylindole (DAPI). Pictures were taken by a Nikon Eclipse E600 microscope with the help of Lucia Cytogenetics version 1.5.6 program, or by a confocal laser scanning microscope (MRC-1024, Bio-Rad Richmond, CA). Details of antibodies and their appropriate dilutions are found in Supplementary Table 1.

4.5. Phospho-RTK array and Western blot

Total proteins were extracted from frozen liver tissues. After homogenization in liquid nitrogen 1 ml of lysis buffer was added to the samples (20 mM TRIS pH 7.5, 2 mM EDTA, 150 mM NaCl, 1% Triton-X100, 0.5% Protease Inhibitor Cocktail (Sigma, St. Luis, MO) 2 mM Na_3VO_4, 10 mM NaF). After incubation for 30 min on ice, samples were centrifuged at 15,000 *g* for 20 min. Supernatants were kept and protein concentrations were measured as described before by Bradford (1976). The activities of phospho-receptor tyrosine kinases (Phospho-RTKs) were assessed by their relative levels of phosphorylation using the Proteome Profiler Array (R&D Systems, Minneapolis, MN, USA) according to the manufacturer's instructions. Pooled samples of five livers from the same experimental group were homogenized in lysis buffer (described above) and adjusted to 1.2 μg protein/μl lysate. Signals were developed by incubating the membrane in SuperSignal West Pico Chemiluminescent Substrate Kit (Pierce/Thermo Scientific, Waltham, MA), and visualized on a Kodak Image Station 4000MM Digital Imaging System.

For Western blot, 30 μg of total proteins was mixed with loading buffer containing β-mercaptoethanol and was incubated at 99 °C for 5 min. Denatured samples were loaded onto a 10% polyacrylamide gel and were run for 30 min at 200 V on a Mini Protean vertical electrophoresis equipment (Bio-Rad, Hercules, CA). Proteins were transferred to PVDF membrane (Millipore, Billerica, MA) by blotting for 1.5 h at 100 V. Ponceau staining was applied to determine blotting efficiency. Membranes were blocked with 3 w/v% non-fat dry milk (Bio-Rad) in TBS for 1 h followed by incubation with the primary antibodies at 4 °C for 16 h. Ponceau staining served as loading control. Membranes were washed 5 times with TBS containing 0.05 v/v% Tween-20, then were incubated with appropriate secondary antibodies for 1 h. Signals were detected by SuperSignal West Pico Chemiluminescent Substrate Kit (Pierce/Thermo Scientific), and visualized by Kodak Image Station 4000MM Digital Imaging System. Western blot analyses were performed 3 independent times, running the samples in duplicates. The density of the bands was measured by the Kodak Image Station. For antibody specifications and dilutions applied see Supplementary Table 1.

4.6. Statistical analysis

All statistical analyses were made with GraphPad Prism 4.03 software (Graphpad Software Inc.). Data were tested for normal distribution by D'Agostino and Pearson's omnibus normality test. Significance of changes was tested by non-parametric tests (Mann–Whitney) or Students' *t*-tests depending on the distribution of the data. The difference between wild type and $Dcn^{-/-}$ groups in tumor prevalence was tested for significance by χ^2-test. The independent experimental sets were compared for reproducibility. Only reproducible significant changes were considered as significant. Significance was declared at the standard $p < 0.05$ level.

Supplementary data to this article can be found online at http://dx.doi.org/10.1016/j.matbio.2013.11.004.

Acknowledgment

This work was supported in part by Hungarian Scientific Research Fund, grants 67925 and 100904 (to IK); grant 105763 (to KB), and by the National Institutes of Health grant RO1 CA39481 (to RVI). The authors would like to thank András Sztodola and Mónika Borza for

their help with animal experiments and for Zsuzsa Kaminszky for her technical assistance.

References

Araki, K., Wakabayashi, H., Shintani, K., Morikawa, J., Matsumine, A., Kusuzaki, K., Sudo, A., Uchida, A., 2009. Decorin suppresses bone metastasis in a breast cancer cell line. Oncology 77, 92–99.

Baghy, K., Dezso, K., Laszlo, V., Fullar, A., Peterfia, B., Paku, S., Nagy, P., Schaff, Z., Iozzo, R.V., Kovalszky, I., 2011. Ablation of the decorin gene enhances experimental hepatic fibrosis and impairs hepatic healing in mice. Lab. Invest. 91, 439–451.

Baghy, K., Horvath, Z., Regos, E., Kiss, K., Schaff, Z., Iozzo, R.V., Kovalszky, I., 2013. Decorin interferes with platelet-derived growth factor receptor signaling in experimental hepatocarcinogenesis. FEBS J. 280, 2150–2164.

Becker, F.F., 1983. Thioacetamide hepatocarcinogenesis. J. Natl. Cancer Inst. 71, 553–558.

Berasain, C., Perugorria, M.J., Latasa, M.U., Castillo, J., Goni, S., Santamaria, M., Prieto, J., Avila, M.A., 2009. The epidermal growth factor receptor: a link between inflammation and liver cancer. Exp. Biol. Med. 234, 713–725.

Bertino, G., Ardiri, A., Malaguarnera, M., Malaguarnera, G., Bertino, N., Calvagno, G.S., 2012. Hepatocellular carcinoma serum markers. Semin. Oncol. 39, 410–433.

Bi, X., Tong, C., Dockendorff, A., Bancroft, L., Gallagher, L., Guzman, G., Iozzo, R.V., Augenlicht, L.H., Yang, W., 2008. Genetic deficiency of decorin causes intestinal tumor formation through disruption of intestinal cell maturation. Carcinogenesis 29, 1435–1440.

Bi, X., Pohl, N.M., Qian, Z., Yang, G.R., Gou, Y., Guzman, G., Kajdacsy-Balla, A., Iozzo, R.V., Yang, W., 2012. Decorin-mediated inhibition of colorectal cancer growth and migration is associated with E-cadherin in vitro and in mice. Carcinogenesis 33, 326–330.

Bradford, M.M., 1976. A rapid and sensitive method for the quantitation of microgram quantities of protein utilizing the principle of protein–dye binding. Anal. Biochem. 72, 248–254.

Brandan, E., Gutierrez, J., 2013. Role of skeletal muscle proteoglycans during myogenesis. Matrix Biol. 32, 289–297.

Buraschi, S., Pal, N., Tyler-Rubinstein, N., Owens, R.T., Neill, T., Iozzo, R.V., 2010. Decorin antagonizes Met receptor activity and down-regulates {beta}-catenin and Myc levels. J. Biol. Chem. 285, 42075–42085.

Buraschi, S., Neill, T., Owens, R.T., Iniguez, L.A., Purkins, G., Vadigepalli, R., Evans, B., Schaefer, L., Peiper, S.C., Wang, Z.X., Iozzo, R.V., 2012. Decorin protein core affects the global gene expression profile of the tumor microenvironment in a triple-negative orthotopic breast carcinoma xenograft model. PloS One 7, e45559.

Buraschi, S., Neill, T., Goyal, A., Poluzzi, C., Smythies, J., Owens, R.T., Schaefer, L., Torres, A., Iozzo, R.V., 2013. Decorin causes autophagy in endothelial cells via Peg3. Proc. Natl. Acad. Sci. U. S. A. 110, E2582–E2591.

Camus-Randon, A.M., Raffalli, F., Bereziat, J.C., McGregor, D., Konstandi, M., Lang, M.A., 1996. Liver injury and expression of cytochromes P450: evidence that regulation of CYP2A5 is different from that of other major xenobiotic metabolizing CYP enzymes. Toxicol. Appl. Pharmacol. 138, 140–148.

Chen, S., Birk, D.E., 2013. The regulatory roles of small leucine-rich proteoglycans in extracellular matrix assembly. FEBS J. 280, 2120–2137.

Chen, Q., Seol, D.W., Carr, B., Zarnegar, R., 1997. Co-expression and regulation of Met and Ron proto-oncogenes in human hepatocellular carcinoma tissues and cell lines. Hepatology 26, 59–66.

Chen, X.H., Li, Z.Q., Peng, H., Jin, S.M., Fu, H.Q., Zhu, T.C., Weng, X.G., 2013. Type 1 insulin-like growth factor receptor monoclonal antibody (HX-1162) treatment for liver cancer. OncoTargets Ther. 6, 527–530.

Cho, S.B., Park, Y.L., Song, Y.A., Kim, K.Y., Lee, G.H., Cho, D.H., Myung, D.S., Park, K.J., Lee, W.S., Chung, I.J., Choi, S.K., Kim, K.K., Joo, Y.E., 2011. Small interfering RNA-directed targeting of RON alters invasive and oncogenic phenotypes of human hepatocellular carcinoma cells. Oncol. Rep. 26, 1581–1586.

Csordas, G., Santra, M., Reed, C.C., Eichstetter, I., McQuillan, D.J., Gross, D., Nugent, M.A., Hajnoczky, G., Iozzo, R.V., 2000. Sustained down-regulation of the epidermal growth factor receptor by decorin. A mechanism for controlling tumor growth in vivo. J. Biol. Chem. 275, 32879–32887.

Dahmani, R., Just, P.A., Perret, C., 2011. The Wnt/beta-catenin pathway as a therapeutic target in human hepatocellular carcinoma. Clinics and research in hepatology and gastroenterology 35. 709–713.

Daley, W.P., Peters, S.B., Larsen, M., 2008. Extracellular matrix dynamics in development and regenerative medicine. J. Cell Sci. 121, 255–264.

Danielson, K.G., Baribault, H., Holmes, D.F., Graham, H., Kadler, K.E., Iozzo, R.V., 1997. Targeted disruption of decorin leads to abnormal collagen fibril morphology and skin fragility. J. Cell Biol. 136, 729–743.

Danilkovitch-Miagkova, A., Miagkov, A., Skeel, A., Nakaigawa, N., Zbar, B., Leonard, E.J., 2001. Oncogenic mutants of RON and MET receptor tyrosine kinases cause activation of the beta-catenin pathway. Mol. Cell. Biol. 21, 5857–5868.

De Luca, A., Santra, M., Baldi, A., Giordano, A., Iozzo, R.V., 1996. Decorin-induced growth suppression is associated with up-regulation of p21, an inhibitor of cyclin-dependent kinases. J. Biol. Chem. 271, 18961–18965.

Dudas, J., Kovalszky, I., Gallai, M., Nagy, J.O., Schaff, Z., Knittel, T., Mehde, M., Neubauer, K., Szalay, F., Ramadori, G., 2001. Expression of decorin, transforming growth factor-beta 1, tissue inhibitor metalloproteinase 1 and 2, and type IV collagenases in chronic hepatitis. Am. J. Clin. Pathol. 115, 725–735.

Dunkman, A.A., Buckley, M.R., Mienaltowski, M.J., Adams, S.M., Thomas, S.J., Satchell, L., Kumar, A., Pathmanathan, L., Beason, D.P., Iozzo, R.V., Birk, D.E., Soslowsky, L.J., 2013. Decorin expression is important for age-related changes in tendon structure and mechanical properties. Matrix Biol. 32, 3–13.

El-Serag, H.B., Rudolph, K.L., 2007. Hepatocellular carcinoma: epidemiology and molecular carcinogenesis. Gastroenterology 132, 2557–2576.

Farber, E., 1984. The multistep nature of cancer development. Cancer Res. 44, 4217–4223.

Ferdous, Z., Peterson, S.B., Tseng, H., Anderson, D.K., Iozzo, R.V., Grande-Allen, K.J., 2010. A role for decorin in controlling proliferation, adhesion, and migration of murine embryonic fibroblasts. J. Biomed. Mater. Res. A 93, 419–428.

Goldoni, S., Seidler, D.G., Heath, J., Fassan, M., Baffa, R., Thakur, M.L., Owens, R.T., McQuillan, D.J., Iozzo, R.V., 2008. An antimetastatic role for decorin in breast cancer. Am. J. Pathol. 173, 844–855.

Goldoni, S., Humphries, A., Nystrom, A., Sattar, S., Owens, R.T., McQuillan, D.J., Ireton, K., Iozzo, R.V., 2009. Decorin is a novel antagonistic ligand of the Met receptor. J. Cell Biol. 185, 743–754.

Grimes, C.A., Jope, R.S., 2001. The multifaceted roles of glycogen synthase kinase 3beta in cellular signaling. Prog. Neurobiol. 65, 391–426.

Guo, J., Friedman, S.L., 2007. Hepatic fibrogenesis. Sem. Liver Dis. 27, 413–426.

Harper, J.W., Adami, G.R., Wei, N., Keyomarsi, K., Elledge, S.J., 1993. The p21 Cdk-interacting protein Cip1 is a potent inhibitor of G1 cyclin-dependent kinases. Cell 75, 805–816.

Harper, J.W., Elledge, S.J., Keyomarsi, K., Dynlacht, B., Tsai, L.H., Zhang, P., Dobrowolski, S., Bai, C., Connell-Crowley, L., Swindell, E., et al., 1995. Inhibition of cyclin-dependent kinases by p21. Mol. Biol. Cell 6, 387–400.

He, T.C., Sparks, A.B., Rago, C., Hermeking, H., Zawel, L., da Costa, L.T., Morin, P.J., Vogelstein, B., Kinzler, K.W., 1998. Identification of c-MYC as a target of the APC pathway. Science 281, 1509–1512 (New York, N.Y.).

Heindryckx, F., Colle, I., Van Vlierberghe, H., 2009. Experimental mouse models for hepatocellular carcinoma research. Int. J. Exp. Pathol. 90, 367–386.

Hielscher, A.C., Qiu, C., Gerecht, S., 2012. Breast cancer cell-derived matrix supports vascular morphogenesis. Am. J. Physiol. Cell Physiol. 302, C1243–C1256.

Hu, T., Li, C., 2010. Convergence between Wnt-beta-catenin and EGFR signaling in cancer. Mol. Cancer 9, 236.

Hu, Y., Sun, H., Owens, R.T., Wu, J., Chen, Y.Q., Berquin, I.M., Perry, D., O'Flaherty, J.T., Edwards, I.J., 2009. Decorin suppresses prostate tumor growth through inhibition of epidermal growth factor and androgen receptor pathways. Neoplasia 11, 1042–1053.

Hynes, R.O., 2009. The extracellular matrix: not just pretty fibrils. Science 326, 1216–1219 (New York, N.Y.).

Ichii, M., Frank, M.B., Iozzo, R.V., Kincade, P.W., 2012. The canonical Wnt pathway shapes niches supportive of hematopoietic stem/progenitor cells. Blood 119, 1683–1692.

Iozzo, R.V., 1999. The biology of the small leucine-rich proteoglycans. Functional network of interactive proteins. J. Biol. Chem. 274, 18843–18846.

Iozzo, R.V., Cohen, I., 1993. Altered proteoglycan gene expression and the tumor stroma. Experientia 49, 447–455.

Iozzo, R.V., Murdoch, A.D., 1996. Proteoglycans of the extracellular environment: clues from the gene and protein side offer novel perspectives in molecular diversity and function. Faseb J. 10, 598–614.

Iozzo, R.V., Sanderson, R.D., 2011. Proteoglycans in cancer biology, tumour microenvironment and angiogenesis. J. Cell. Mol. Med. 15, 1013–1031.

Iozzo, R.V., Schaefer, L., 2010. Proteoglycans in health and disease: novel regulatory signaling mechanisms evoked by the small leucine-rich proteoglycans. FEBS J. 277, 3864–3875.

Iozzo, R.V., Chakrani, F., Perrotti, D., McQuillan, D.J., Skorski, T., Calabretta, B., Eichstetter, I., 1999a. Cooperative action of germ-line mutations in decorin and p53 accelerates lymphoma tumorigenesis. Proc. Natl. Acad. Sci. U. S. A. 96, 3092–3097.

Iozzo, R.V., Moscatello, D.K., McQuillan, D.J., Eichstetter, I., 1999b. Decorin is a biological ligand for the epidermal growth factor receptor. J. Biol. Chem. 274, 4489–4492.

Iozzo, R.V., Buraschi, S., Genua, M., Xu, S.Q., Solomides, C.C., Peiper, S.C., Gomella, L.G., Owens, R.C., Morrione, A., 2011. Decorin antagonizes IGF receptor I (IGF-IR) function by interfering with IGF-IR activity and attenuating downstream signaling. J. Biol. Chem. 286, 34712–34721.

Jacobs, K.M., Bhave, S.R., Ferraro, D.J., Jaboin, J.J., Hallahan, D.E., Thotala, D., 2012. GSK-3beta: a bifunctional role in cell death pathways. Int. j. cell biol. 2012, 930710.

Jain, S., Singhal, S., Lee, P., Xu, R., 2010. Molecular genetics of hepatocellular neoplasia. Am. J. Transl. Res. 2, 105–118.

Jarvelainen, H., Sainio, A., Koulu, M., Wight, T.N., Penttinen, R., 2009. Extracellular matrix molecules: potential targets in pharmacotherapy. Pharmacol. Rev. 61, 198–223.

Jung, P., Hermeking, H., 2009. The c-MYC-AP4-p21 cascade. Cell cycle 8, 982–989.

Khan, G.A., Girish, G.V., Lala, N., Di Guglielmo, G.M., Lala, P.K., 2011. Decorin is a novel VEGFR-2-binding antagonist for the human extravillous trophoblast. Mol. Endocrinol. 25, 1431–1443.

Lee, J.S., Thorgeirsson, S.S., 2002. Functional and genomic implications of global gene expression profiles in cell lines from human hepatocellular cancer. Hepatology 35, 1134–1143.

Lempinen, M., Lyytinen, I., Nordin, A., Tervahartiala, T., Makisalo, H., Sorsa, T., Isoniemi, H., 2013. Prognostic value of serum MMP-8, -9 and TIMP-1 in patients with hepatocellular carcinoma. Ann. Med. 45, 482–487.

Li, Y., Liu, Y., Xia, W., Lei, D., Voorhees, J.J., Fisher, G.J., 2013. Age-dependent alterations of decorin glycosaminoglycans in human skin. Sci. Rep. 3, 2422.

Llovet, J.M., Burroughs, A., Bruix, J., 2003. Hepatocellular carcinoma. Lancet 362, 1907–1917.

Loeppen, S., Schneider, D., Gaunitz, F., Gebhardt, R., Kurek, R., Buchmann, A., Schwarz, M., 2002. Overexpression of glutamine synthetase is associated with beta-catenin-mutations in mouse liver tumors during promotion of hepatocarcinogenesis by phenobarbital. Cancer Res. 62, 5685–5688.

Lu, J.W., Lin, Y.M., Chang, J.G., Yeh, K.T., Chen, R.M., Tsai, J.J., Su, W.W., Hu, R.M., 2013. Clinical implications of deregulated CDK4 and Cyclin D1 expression in patients with human hepatocellular carcinoma. Med. Oncol. 30, 379.

Marastoni, S., Ligresti, G., Lorenzon, E., Colombatti, A., Mongiat, M., 2008. Extracellular matrix: a matter of life and death. Connect. Tissue Res. 49, 203–206.

Merline, R., Moreth, K., Beckmann, J., Nastase, M.V., Zeng-Brouwers, J., Tralhao, J.G., Lemarchand, P., Pfeilschifter, J., Schaefer, R.M., Iozzo, R.V., Schaefer, L., 2011. Signaling by the matrix proteoglycan decorin controls inflammation and cancer through PDCD4 and MicroRNA-21. Sci. Signal. 4, ra75.
Morrione, A., Neill, T., Iozzo, R.V., 2013. Dichotomy of decorin activity on the insulin-like growth factor-I system. FEBS J. 280, 2138–2149.
Neill, T., Painter, H., Buraschi, S., Owens, R.T., Lisanti, M.P., Schaefer, L., Iozzo, R.V., 2012a. Decorin antagonizes the angiogenic network: concurrent inhibition of Met, hypoxia inducible factor 1alpha, vascular endothelial growth factor A, and induction of thrombospondin-1 and TIMP3. J. Biol. Chem. 287, 5492–5506.
Neill, T., Schaefer, L., Iozzo, R.V., 2012b. Decorin: a guardian from the matrix. Am. J. Pathol. 181, 380–387.
Neill, T., Jones, H.R., Crane-Smith, Z., Owens, R.T., Schaefer, L., Iozzo, R.V., 2013. Decorin induces rapid secretion of thrombospondin-1 in basal breast carcinoma cells via inhibition of Ras homolog gene family, member A/Rho-associated coiled-coil containing protein kinase 1. FEBS J. 280, 2353–2368.
Nikitovic, D., Aggelidakis, J., Young, M.F., Iozzo, R.V., Karamanos, N.K., Tzanakakis, G.N., 2012. The biology of small leucine-rich proteoglycans in bone pathophysiology. J. Biol. Chem. 287, 33926–33933.
Nystrom, A., Shaik, Z.P., Gullberg, D., Krieg, T., Eckes, B., Zent, R., Pozzi, A., Iozzo, R.V., 2009. Role of tyrosine phosphatase SHP-1 in the mechanism of endorepellin angiostatic activity. Blood 114, 4897–4906.
Okazaki, I., Inagaki, Y., 2012. Novel strategies for hepatocellular carcinoma based on MMPs science. Anti Cancer Agents Med. Chem. 12, 753–763.
Oseini, A.M., Roberts, L.R., 2009. PDGFRalpha: a new therapeutic target in the treatment of hepatocellular carcinoma? Expert Opin. Ther. Targets 13, 443–454.
Reed, C.C., Iozzo, R.V., 2002. The role of decorin in collagen fibrillogenesis and skin homeostasis. Glycoconj. J. 19, 249–255.
Reed, C.C., Gauldie, J., Iozzo, R.V., 2002. Suppression of tumorigenicity by adenovirus-mediated gene transfer of decorin. Oncogene 21, 3688–3695.
Reed, C.C., Waterhouse, A., Kirby, S., Kay, P., Owens, R.T., McQuillan, D.J., Iozzo, R.V., 2005. Decorin prevents metastatic spreading of breast cancer. Oncogene 24, 1104–1110.
Rivadeneira, D.B., Mayhew, C.N., Thangavel, C., Sotillo, E., Reed, C.A., Grana, X., Knudsen, E.S., 2010. Proliferative suppression by CDK4/6 inhibition: complex function of the retinoblastoma pathway in liver tissue and hepatoma cells. Gastroenterology 138, 1920–1930.
Robinson, P.S., Huang, T.F., Kazam, E., Iozzo, R.V., Birk, D.E., Soslowsky, L.J., 2005. Influence of decorin and biglycan on mechanical properties of multiple tendons in knockout mice. J. Biomech. Eng. 127, 181–185.
Rozario, T., DeSimone, D.W., 2010. The extracellular matrix in development and morphogenesis: a dynamic view. Dev. Biol. 341, 126–140.
Ruoslahti, E., Yamaguchi, Y., 1991. Proteoglycans as modulators of growth factor activities. Cell 64, 867–869.
Santra, M., Mann, D.M., Mercer, E.W., Skorski, T., Calabretta, B., Iozzo, R.V., 1997. Ectopic expression of decorin protein core causes a generalized growth suppression in neoplastic cells of various histogenetic origin and requires endogenous p21, an inhibitor of cyclin-dependent kinases. J. Clin. Invest. 100, 149–157.
Schaefer, L., Iozzo, R.V., 2012. Small leucine-rich proteoglycans, at the crossroad of cancer growth and inflammation. Curr. Opin. Genet. Dev. 22, 56–57.
Schaefer, L., Tsalastra, W., Babelova, A., Baliova, M., Minnerup, J., Sorokin, L., Grone, H.J., Reinhardt, D.P., Pfeilschifter, J., Iozzo, R.V., Schaefer, R.M., 2007. Decorin-mediated regulation of fibrillin-1 in the kidney involves the insulin-like growth factor-I receptor and mammalian target of rapamycin. Am. J. Pathol. 170, 301–315.
Schonherr, E., Sunderkotter, C., Iozzo, R.V., Schaefer, L., 2005. Decorin, a novel player in the insulin-like growth factor system. J. Biol. Chem. 280, 15767–15772.
Seidler, D.G., 2012. The galactosaminoglycan-containing decorin and its impact on diseases. Curr. Opin. Struct. Biol. 22, 578–582.
Seidler, D.G., Dreier, R., 2008. Decorin and its galactosaminoglycan chain: extracellular regulator of cellular function? IUBMB life 60, 729–733.
Seidler, D.G., Mohamed, N.A., Bocian, C., Stadtmann, A., Hermann, S., Schafers, K., Schafers, M., Iozzo, R.V., Zarbock, A., Gotte, M., 2011. The role for decorin in delayed-type hypersensitivity. J. Immunol. 187, 6108–6119.
Sengupta, B., Siddiqi, S.A., 2012. Hepatocellular carcinoma: important biomarkers and their significance in molecular diagnostics and therapy. Curr. Med. Chem. 19, 3722–3729.
Sherman, M., 2010. Epidemiology of hepatocellular carcinoma. Oncology 78 (Suppl. 1), 7–10.
Sofeu Feugaing, D.D., Gotte, M., Viola, M., 2013. More than matrix: the multifaceted role of decorin in cancer. Eur. J. Cell Biol. 92, 1–11.
Stock, P., Monga, D., Tan, X., Micsenyi, A., Loizos, N., Monga, S.P., 2007. Platelet-derived growth factor receptor-alpha: a novel therapeutic target in human hepatocellular cancer. Mol. Cancer Ther. 6, 1932–1941.
Tralhao, J.G., Schaefer, L., Micegova, M., Evaristo, C., Schonherr, E., Kayal, S., Veiga-Fernandes, H., Danel, C., Iozzo, R.V., Kresse, H., Lemarchand, P., 2003. In vivo selective and distant killing of cancer cells using adenovirus-mediated decorin gene transfer. Faseb J. 17, 464–466.
Villanueva, A., Newell, P., Chiang, D.Y., Friedman, S.L., Llovet, J.M., 2007. Genomics and signaling pathways in hepatocellular carcinoma. Sem. Liver Dis. 27, 55–76.
Whittaker, S., Marais, R., Zhu, A.X., 2010. The role of signaling pathways in the development and treatment of hepatocellular carcinoma. Oncogene 29, 4989–5005.
Wu, J., Zhu, A.X., 2011. Targeting insulin-like growth factor axis in hepatocellular carcinoma. J. Hematol. Oncol. 4, 30.
Yamaguchi, Y., Mann, D.M., Ruoslahti, E., 1990. Negative regulation of transforming growth factor-beta by the proteoglycan decorin. Nature 346, 281–284.
Zhang, G., Chen, S., Goldoni, S., Calder, B.W., Simpson, H.C., Owens, R.T., McQuillan, D.J., Young, M.F., Iozzo, R.V., Birk, D.E., 2009. Genetic evidence for the coordinated regulation of collagen fibrillogenesis in the cornea by decorin and biglycan. J. Biol. Chem. 284, 8888–8897.
Zhang, Y., Wang, Y., Du, Z., Wang, Q., Wu, M., Wang, X., Wang, L., Cao, L., Hamid, A.S., Zhang, G., 2012. Recombinant human decorin suppresses liver HepG2 carcinoma cells by p21 upregulation. OncoTargets Ther. 5, 143–152.
Zhu, J.X., Goldoni, S., Bix, G., Owens, R.T., McQuillan, D.J., Reed, C.C., Iozzo, R.V., 2005. Decorin evokes protracted internalization and degradation of the epidermal growth factor receptor via caveolar endocytosis. J. Biol. Chem. 280, 32468–32479.